Article

J. Biol. Regul. Homeost. Agents. 2024; 38(7): 5537–5550
https://doi.org/10.23812/j.biol.regul.homeost.agents.20243807.445

Biogenic Silver Nanoparticles Combined with L-Arginine Using *Escherichia coli* and their Antibacterial and Cytotoxic Activities via ROS Production against A-549 Cells

Khairunnisa Imanina M Binti Nazaruddin[1], Shahnaz Majeed[1,*], Mohammed Danish[2], Mohamad Nasir Mohamad Ibrahim[3], Sreenivas Patro Sisinthy[1], Mohammed Tahir Ansari[4], Ravindran Muthukumarasamy[1], Ali Mohammed Alalawi[5], El-Refaie Kenawy[6], Saad Alkahtani[7], Mohammed Al-Zharani[8], Nada H. Aljarba[9], Md Saquib Hasnain[10,*]

[1]Faculty of Pharmacy and Health Sciences, Universiti Kuala Lumpur, Royal College of Medicine, 30450 Ipoh Perak, Malaysia
[2]Bioresource Technology Division, School of Industrial Technology, Universiti Sains Malaysia, 11800 Penang, Malaysia
[3]Material Technology Research Group (MaTRec) School of Chemical Sciences, Universiti Sains Malaysia, 11800 Penang, Malaysia
[4]Faculty of Science and Engineering, School of Pharmacy, University of Nottingham Malaysia, Semenyih, 43500 Selangor, Malaysia
[5]Department of Pharmacology and Toxicology, College of Pharmacy, Taibah University, 42353 Madinah, Saudi Arabia
[6]Polymer Research Group, Chemistry Department, Faculty of Science, Tanta University, 31527 Tanta, Egypt
[7]Department of Zoology, College of Science, King Saud University, P. O. Box 2455, Riyadh-11451, Saudi Arabia
[8]Department of Biology, College of Science, Imam Mohammad Ibn Saud Islamic University (IMSIU), 11623 Riyadh, Saudi Arabia
[9]Department of Biology, College of Science, Princess Nourah bint Abdulrahman University, P. O. Box 84428, Riyadh-11671, Saudi Arabia
[10]Department of Pharmacy, Palamau Institute of Pharmacy, Chianki, Daltonganj, 822102 Jharkhand, India
*Correspondence: Shahnazmajeed5@gmail.com (Shahnaz Majeed); msaquibhasnain@gmail.com (Md Saquib Hasnain)
Submitted: 23 September 2023 Revised: 27 November 2023 Accepted: 11 December 2023 Published: 1 July 2024

Background: Silver and its nanoparticles have gained attention owing to their unique physicochemical properties which contribute to their antimicrobial and anticancer properties. The primary focus of this study was the synthesis of silver nanoparticles (AgNPs) using the cell filtrate of *Escherichia coli* (*E. coli*) American Type Culture Collection (ATCC) 8739.

Methods: Silver nanoparticles were synthesized using *E. coli* and coated with non-toxic, naturally occurring L-arginine. L-arginine-coated AgNPs (L-AgNPs) were tested for purity, elemental composition, morphology, topology, and stability. Subsequently, they were tested for their antibacterial, apoptotic, reactive oxygen species (ROS), and cytotoxic effects on A549 lung cancer cells using the 3-(4,5-Dimethylthiazol-2-yl)-2,5-diphenyltetrazolium bromide (MTT) assay.

Results: The study revealed the formation of well-defined nanoparticles with a spherical shape, falling within the size range of 8.8 nm to 44.6 nm. The L-AgNPs exhibited significant antibacterial characteristics, with the largest zone of inhibition observed against *Salmonella* spp. (18.7 $\pm$ 0.9 mm) and the smallest against *Bacillus cereus* (8.7 $\pm$ 0.9 mm). The half maximal inhibitory concentration (IC_{50}) value of L-AgNPs against A549 lung cancer cells was 58.67 µg/mL, while against 3T3-L1 cells, it was measured as 98.03 µg/mL via MTT assay. L-AgNPs induced apoptosis, as confirmed by morphological alterations in the cells, membrane blebbing, and chromatin condensation. These nanoparticles also triggered the production of reactive oxygen species (ROS) due to cellular oxidative stress, as indicated by the increased levels of dichlorodihydrofluorescein (DCF).

Conclusion: This research demonstrates the potential application of these L-AgNPs in the biotechnology and pharmaceutical industries for their antibacterial and anticancer properties.

Keywords: L-AgNPs; MTT assay; antibacterial; ROS; lung cancer

Introduction

Nanotechnology has expanded its applications across various sectors with the ability to work with materials in 1 to 100 nm size range. Strategies for effective therapeutic drug administration include implementing the emerging field of nanotechnology to suitable targets for better efficacy and safety [1]. Nanoparticles have immense applications in various fields, such as vaccines, drug therapy, and cancer treatment, and have attracted the attention of many researchers [2]. Functionalization of nanoparticles by surface modification enhances their availability and reduces toxicity, with unique applications in biomedicine [3].

The increasing prevalence of antimicrobial resistance (AMR) in the modern era has become a significant public health concern. It poses a significant challenge in effec-

Journal of
BIOLOGICAL REGULATORS
and Homeostatic Agents

tively combating and managing various infections caused by microorganisms as they have become resistant to conventional treatments [2]. Additionally, patients may be incapable of withstanding high doses of antibiotics even when conventional doses seem ineffective due to resistance. The development of resistance in bacterial pathogens alerts the medical fraternity and researchers to develop or search for new antibacterial agents capable of countering this resistance and shift their focus to applying nanomaterials.

Nanomaterials derived from metals have a large surface area, allowing them to be effective antibacterial agents, even when used in small concentrations [3]. Combining nanoparticles with antibiotics or other nanomaterials has also enhanced antibacterial activity [4]. Metallic nanoparticles, such as silver nanoparticles (AgNPs), lack specific receptor binding to bacterial cells, impeding antibiotic resistance development and broadening their antibacterial efficacy [5].

Lung cancer, also known as lung carcinoma, is characterized by the unrestricted growth of the lung tissues [6,7]. The treatment modalities for metastatic lung cancer include surgical intervention, radiation therapy, and chemotherapy [8–10]. However, chemotherapy damages the tumor cells and is toxic to healthy cells, especially rapidly growing cells like the intestines, stomach, mouth, and blood cells throughout the body [11]. Nanoparticles also possess anticancer capabilities, with limited side effects compared to chemotherapy drugs, as they may extend or modify the drug release and improve bioavailability [12]. Silver nanoparticles nowadays have been explored immensely due to their diverse chemical, physical, and optical properties [13]. AgNPs are known to exhibit antibacterial and anticancer activities. They have been reported to exert inhibitory effects on cell signaling pathways, particularly those involved in cancer progression, and selectively inhibit tumor growth [14]. These substances have been observed to elicit oxidative stress within cells, resulting in the release of free radicals that contribute to cellular damage and ultimately culminate in cell death. Silver nanoparticles are also used in food containers and as an antiseptic for cleaning surgical instruments andcatheters [15,16]. The fusion of nanoparticles and biomolecules could work as an "efficient ornament" for bioengineering purposes. The nanoparticle stability has been confirmed to be enriched by covalent interaction between the surface of the nanoparticle and capping ligands [17]. Certain capping agents enable the conversion of metal ions, like silver ions, into metallic element-based nanoparticles [18]. The capping of nanoparticles with biological bits may also improve the efficiency of nanoparticles and biological molecules, producing a concurring effect. Furthermore, the capping agents reportedly minimize the aggregation of nanoparticles [19]. Literature also implies nanoparticle capping with biological molecules would synthesis a highly precise nanodrug delivery system with diverse biomedicine applications.

The method of creating nanoparticles through organic biological agents like fungi, bacteria, and plant extracts is referred to as "green synthesis of nanoparticles" [20]. There are chemical, physical, and biological techniques to synthesize AgNPs. Chemical and physical methods are subject to substantial time consumption and use of potentially hazardous chemicals. Conversely, a biological method has demonstrated its efficacy as a straightforward, economically viable, and environmentally sustainable method [21]. Biological organisms such as fungi, algae, plants, and bacteria act as "nanofactories" by reducing metal ions into metallic nanoparticles. Bacterial cell filtrates are an excellent source for reduction because they contain many enzymes. The interaction between silver ions and bacteria determines the size and structure of AgNPs produced by microorganisms [22].

This study proposes an alternative antibacterial and anticancer agent characterized by low toxicity towards normal cells and the ability to demonstrate synergistic effects. This approach aims to reduce the potential development of antimicrobial resistance against conventional antibacterial agents. Silver nanoparticles were selected as the metallic nanoparticles to be studied since silver has been widely recognized as a potent broad-spectrum antibacterial or as having inhibitory characteristics against multidrug-resistant bacteria [23,24]. Silver nanoparticles were synthesized using *Escherichia coli* and then coated with nontoxic, naturally occurring L-arginine [23,24]. Arginine is known to improve antibacterial and cytotoxic activities [25] and to minimise toxicity when combined with AgNPs [26]. The L-arginine-coated AgNPs (L-AgNPs) were characterized by their macro and microscopic features. They were then examined for their antibacterial, apoptotic, reactive oxygen species (ROS) determination, and cytotoxic effects against A549 lung cancer cells using 3-(4,5-Dimethylthiazol-2-yl)-2,5-diphenyltetrazolium bromide (MTT).

Materials and Methods

Collection of Bacteria: Cell Lines and Reagents

Silver nitrate ($AgNO_3$, 209139), fetal bovine serum (FBS, F0926), Dulbecco's Modified Eagle Medium-low glucose, nutrient agar media, and MTT (TS191) reagent were obtained from Himedia (Thane, India). DMSO (D8418) was procured from Sigma Aldrich (Mumbai, India). Gentamicin, meropenem, vancomycin, cefotaxime, tetracycline, and erythromycin were acquired from an Oxoid NWAS, Malaysia.

The bacteria *Bacillus cereus* (clinical isolates Malaysia), *Salmonella typhimurium* (clinical isolates Malaysia), *Escherichia coli* American Type Culture Collection (ATCC) 8739, *Pseudomonas aeruginosa* ATCC 9022, and *Staphylococcus aureus* ATCC 33682 were obtained from the American Type Culture Collection (ATCC) Malaysia. The A549 lung carcinoma cells and

3T3-L1 mouse embryonic fibroblast cells were sourced from the National Centre for Cell Science Studies (NCCS) based in Pune, India. The purchased cell lines were grown 2 to 3 times on media to avoid contamination. For further validation we use agar and broth culture method for myoplasm testing.

Biological Synthesis of Silver Nanoparticles

Nutrient agar broth (2.6 g) was added to distilled water (200 mL) in an Erlenmeyer flask to dissolve the agar. The covered Erlenmeyer flasks were autoclaved for 20 minutes at 121 °C. After autoclaving, the broth was cooled, and one loop of *Escherichia coli* (*E. coli*) was added. The Erlenmeyer flask was then incubated at 37 °C overnight to allow the bacteria to grow. After incubation, the Erlenmeyer flask was removed, sonicated at 53 kHz and centrifuged at 4000 rpm for 15 minutes. Following centrifugation, the pellets were discarded, and the supernatant was collected. Subsequently, 1 mM $AgNO_3$ was introduced to the cell filtrate and kept on an orbital shaker in the dark for 24 hours for reduction [27]. The solution was monitored for any color change, which would signify the formation of nanoparticles. Subsequently, the nanoparticle solution underwent centrifugation at 10,000 rpm for 10 minutes and pellets were washed three to four times with distilled water to remove the bacterial debris. The pellets were dried out and used to cap with L-arginine.

Capping of Silver Nanoparticles with L-Arginine

A solution comprising a 1% weight/volume concentration of L-arginine was introduced into a 50 mL volume of silver nanoparticle solution. The solution was incubated for 5 minutes, followed by continuous agitation for 2 hours at room temperature. The confirmation of conjugation was achieved through spectrophotometric analysis within the wavelength range of 300–600 nm, utilizing a Ultraviolet-Visible Spectrophotometer (UV)-visible spectrophotometer (1900, Shimadzu, Selangor, Malaysia). The utilized methodology was derived from the approach developed by Clausen *et al*. 2019 [28], with certain modifications made to suit the requisites of the present investigation.

Characterization of L-Arginine-Capped Silver Nanoparticles

Fourier Transform Infrared (FT-IR) Analysis

The FT-IR spectrophotometer (ShimadzuIRPrestige21, SHIMADZU CORPORATION, Kyoto, Japan) identified functional groups linked with AgNPs and L-AgNPs. A sample of 1 mg was weighed, grinded, and mixed with oven-dried potassium bromide (0.1 g) in a mortar until a homogenous mixture was formed. The combination was compressed as a pellet using a manual benchtop pellet press (46992-0544, Carver, Wabash, IL, USA). After compression, a thin plate sample was placed in the Fourier transform infrared (FT-IR) for further analysis. FT-IR spectra were obtained by scanning AgNPs from 4000 to 400 cm^{-1} with 32 scans and a resolution of 4.0 [29].

Scanning Electron Microscopy (SEM) and Energy-Dispersive X-ray Spectroscopy (EDX) Analysis

The size distribution, morphology, and shape of the synthesized AgNPs were analysed using Scanning Electron Microscopy (SEM), Carl Zeiss Leo Supra 50 VP Field Emission equipped with Oxford INCA-X energy dispersive microanalysis system, Zeiss, Oberkochen, Germany. A dry sample of AgNPs was additionally desiccated and coated with gold to verify the elemental nature of the metal. EDX established the elemental nature of the AgNPs.

Transmission Electron Microscopy (TEM) Analysis

The distribution and morphology of L-arginine-capped AgNPs were examined using TEM. To prepare the sample, the L-AgNPs suspension was sonicated for 5 min to break up agglomerates and evenly distribute the particles. A TEM carbon-coated copper grid was held in place using forceps. Subsequently, a small quantity of the L-AgNPs sample was introduced onto the grid and left to desiccate under ambient conditions. The excess liquid was eliminated using filter paper, and the grid was inserted into a specimen holder for viewing in a highly magnified image [30].

Thermal Gravimetric Analysis (TGA)

The AgNP thermostability and volatile constituents were analysed using TGA (PerkinElmer Thermal Analyzer STA 6000, School of chemical science university sains Malaysia, Penang, Malaysia). AgNP (6.5 ± 1.5 mg) was heated at 20 °C per minute on an aluminium pan under the nitrogen flow. The mass degradation was observed from 30 °C to 900 °C heating at a constant rate [31].

Antibacterial Activity of L-Arginine-Capped Silver Nanoparticles

The antibacterial activity was carried on a nutrient agar medium through the disc diffusion. The petri plates containing the nutrient agar were swabbed with clinically isolated bacterial pathogens *Bacillus cereus*, *Salmonella typhimurium*, *E. coli* ATCC 8739, *Staphylococcus aureus* ATCC 33682, and *Pseudomonas aeruginosa* ATCC 9022. L-arginine-capped and non-capped AgNPs were evaluated on each petri dish using a range of concentrations (10, 20, 30, 40 µg/mL). The positive control employed in the study was levofloxacin. The agar plates were incubated for 12 hours at a temperature of 37 °C. The zone of inhibition around each disc was measured after the incubation period in millimetres.

Journal of
BIOLOGICAL REGULATORS
and Homeostatic Agents

Synergistic Effects of L-Arginine-Capped Silver Nanoparticles against Antibiotics

The synergistic effect of capped and non-capped Ag-NPs by using different antibiotics such as gentamicin (10 µg), vancomycin (30 µg), meropenem (10 µg), cefotaxime (5 µg), tetracycline 30 (µg), and erythromycin (15 µg) against five pathogens was investigated like *Staphylococcus aureus*, *Salmonella typhimurium*, *Bacillus cereus*, *Escherichia coli*, and *Pseudomonas aeruginosa*. The antibiotic disc was impregnated with 20 µg L-AgNPs nanoparticles, and the function was compared with antibiotics alone. The agar plates were exposed to a 12-hour incubation period, after which the inhibition zone was quantified in millimetres.

Cytotoxicity Evaluation through MTT Assay

Cell Line Maintenance

The lung cancer A549 and normal 3T3-L1 cells were cultured at 37 °C under a 5% CO_2 atmosphere in a fresh Dulbecco's Modified Eagle Medium (DMEM) glucose medium supplemented with 1% antibiotic and anti-mycotic solution, and 10% fetal bovine serum. The cells were replenished every 2 days [30,32].

MTT Assay

The A549 lung cancer and 3T3-L1 normal mouse embryonic fibroblast cells were cultivated 96-well with a cell concentration of 20,000 (density) per well. The plates were incubated in a CO_2 incubator for 24 hours. Different concentrations of L-AgNPs, ranging from 10 to 160 µg/mL, were introduced into the wells. Camptothecin (10 µM/mL) was treated as a positive control, and one well was kept as a negative control. Afterwards, the plate was put into an environment with 5% CO_2 concentration at 37 °C for 24 hours. After this incubation, the used media was removed, and a solution containing MTT reagent (0.5 mg/mL) was introduced to the cells. These cells were subsequently shielded from direct light exposure with aluminium foil. The entire plate was placed on a gyratory shaker with gentle agitation for 3 hours. Lastly, a spectrophotometer was used to determine the absorbance of the plate at 570 nm, and cell viability was estimated [33].

% Cell viability = [absorbance of treated cell / absorbance of the untreated cell] × 100

The half maximal inhibitory concentration (IC_{50}) value was calculated using the following formula using a linear regression equation.

$$y = mx + c$$

y is the IC_{50}, and m and c values are taken from the viability graph.

Apoptosis Evaluation through AO/EtBr Staining

The lung cancer cells were cultured on sterile coverslips in a 12-well plate with a poly L-ornithine solution. The cells were spread at 2 × 10^5 cells/2 mL and left for incubation for 24 hours. The lung cancer cells were cultivated on a 12-well plate using sterile coverslips coated with poly L-ornithine. The cells were initially distributed at a quantity of 2 × 10^5 cells/2 mL and afterwards cultured for 24 hours in a CO_2 incubator at a temperature of 37 °C. After incubation, the spent medium was eliminated, and nanoparticles (at their IC_{50} concentration) were applied to cells and positive control and further nurtured for 24 hours in a culture medium (2 mL). Afterwards, plates were washed using phosphate buffer solution (PBS) buffer, and any excess buffer was removed. The staining solution (200 µL) was supplemented, and any excess staining solution was rinsed off with PBS. Subsequently, a small quantity of mounting solution was administered, and the specimens were examined via fluorescence microscopy. The excitation wavelengths of 470/40 nm and 560/40 nm, together with the corresponding wavelengths of 525/50 nm and 645/75 nm for emission, were utilized for the visualization of acridine orange and ethidium bromide, respectively [34]. The image was overlaid with Image J Software v1.48 (LOCI, University of Wisconsin, Madison, WI, USA).

Determination of ROS Using H2DCFDA Staining Method

A549 lung cancer cells were cultured with a density of 0.5 × 10^6 cells/2 mL and incubated in a CO_2 incubator for 24 hours. The spent medium was removed, and PBS wash was performed after incubation. Later, cells were exposed to L-AgNPs at their IC_{50} concentration, along with camptothecin (positive control) and untreated well (negative control). The entire plate was left for incubation for an additional 24 hours.

The culture media was gathered and transferred to 12 × 75 mm polystyrene tubes. After washing with 500 µL of PBS, tubes were nurtured with trypsin-EDTA solution (250 µL). The remaining medium was carefully poured into the corresponding well plate, and cells were recollected in separate 12 × 75 mm polystyrene tubes. After centrifugation at 300 ×g for 5 minutes at 25 °C, the supernatant was discarded, and the pellet was washed through PBS. Next, cells were suspended with 2′,7′-dichlorodihydrofluorescein diacetate (H_2DCFDA) of 10 µM and a cell concentration of 1 × 10^6 cells/mL. This suspension was incubated at 37 °C in the dark for 30 minutes. The cells after incubation were centrifuged at 150 ×g for 5 minutes and the supernatant was carefully separated. Then, cells were resuspended in 400 µL DPBS which was pre-warmed. Flow cytometry analysis was executed through a 488 nm laser for excitation and detection was performed at 535 nm (FL1) for emission [35].

Statistical Analysis

The experimental results were expressed as mean ± Standard deviation (SD) for triplicate determination. The results were analyzed using unpaired *t* test p value < 0.05 was considered statistically significant.

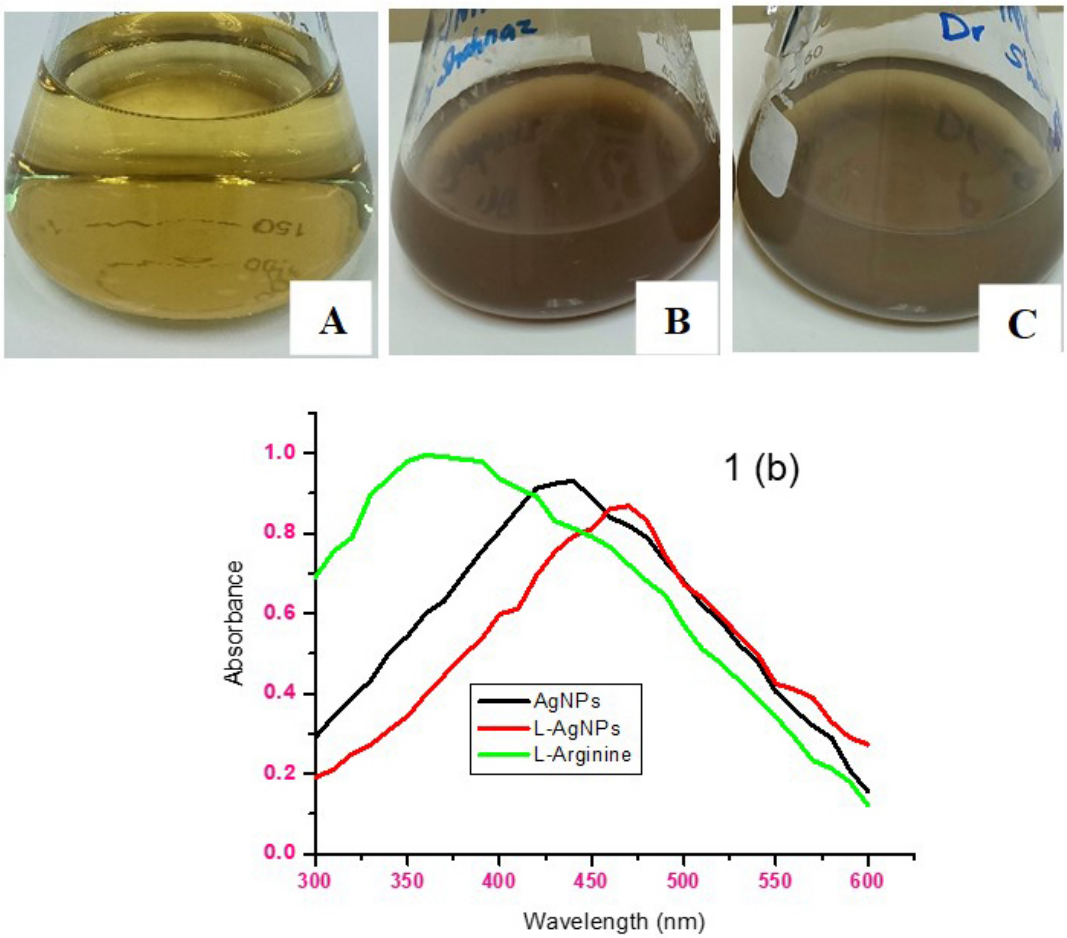

Fig. 1. The UV spectoscopy provides the absorption of nanoparticles which indicates the formation of nanoparticles. (A) *Escherichia coli* (*E. coli*) biomassfiltrate, (B) AgNP, (C) L-AgNPs, (1b) Comparative UV analysis of L-arginine. AgNPs and L-AgNPs show different absorption peaks synthesized from bacterial filtrate. L-AgNPs, L-arginine-coated AgNPs; AgNPs, silver nanoparticles; UV, Ultraviolet-Visible Spectrophotometer.

Results and Discussion

Biosynthesis of Silver Nanoparticles and Capping with L-Arginine

Silver nanoparticles (AgNPs) were synthesized using *E. coli* ATCC 8739. The clear yellow *E. coli* extract solution turned cloudy after overnight incubation, indicating increased *E. coli* bacteria. AgNPs development was indicated by supplementation of $AgNO_3$ to the *E. coli* filtrate from light yellow to dark brown, as revealed in Fig. 1A–C. Fig. 1b shows the comparative UV spectrophotometric analysis of AgNPs, L-AgNPs, and L-arginine with absorption peaks at 418 nm, 470 nm, and 365 nm, respectively which were ascribed to decrease of silver ions and excitation of surface plasmon resonance. The higher peak of L-AgNPs was due to L-arginine grouping with AgNPs [36]. The dark brown color of the L-AgNPs solution was lighter than that of the AgNPs solutions.

Characterization of L-AgNPs

FT-IR Analysis

FT-IR analysis identified the functional groups associated with AgNPs and L-AgNPs, as depicted in Fig. 2. FT-IR spectra of uncapped and capped AgNPs were compared. The prominent functional groups observed in AgNPs are 3360 cm^{-1} corresponding to N-H stretching for aliphatic primary amine, 3194.12 cm^{-1} for alcoholic O-H stretching, 2962.66 cm^{-1} for C-H stretching (alkane), 1662.64 cm^{-1} C=C stretching for alkene, 1568.13 cm^{-1} for stretching of C=O, 1460.11 cm^{-1} for C-H bending (alkane), 1404.18 cm^{-1} for O-H bending of carboxylic acid and two medium intensity peaks at 1128.36 cm^{-1} and 1178.51 cm^{-1} due to stretching of C=O.

For L-AgNPs, the FT-IR curve established a broad peak at 3423.65 cm^{-1} and a weak intensity peak at 2954.59 cm^{-1} due to stretching of O-H for alcohol, two peaks at 1649.14 cm^{-1} and 1394.53 cm^{-1} due to N-H bending of amine and bending of C=O of carboxylic acid, respectively. Other FT-IR peaks were observed at 1111 cm^{-1} for C-

Journal of
BIOLOGICAL REGULATORS
and Homeostatic Agents

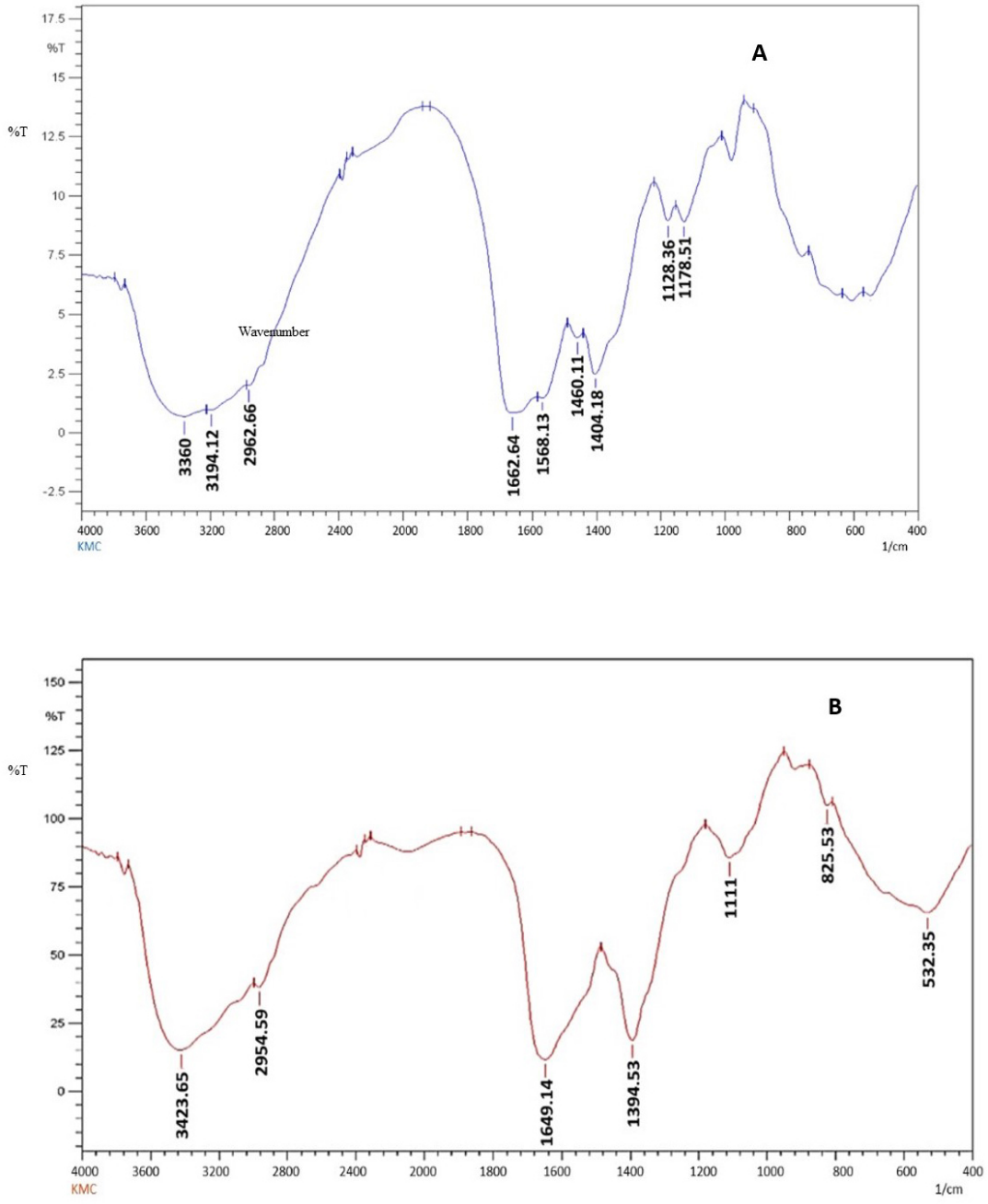

Fig. 2. Fourier transform infrared (FT-IR) spectra of nanoparticles. FT-IR spectra of AgNPs (A); FT-IR spectra of L-AgNPs showing various functional groups linked with nanoparticles (B).

N stretching of amine, 825.53 cm^{-1} for C=C bending of alkene and 532.35 cm^{-1} for C-Br stretching of halo compound.

Previous study has revealed that C=O stretching vibration has been recognized for detecting protein secondary structures [37], proving the existence of L-arginine peptides as a coating agent. Functional groups like amides, amines, alkenes, alkanes, and carbonyl groups, promote biological activity and stability [38]. In AgNPs, the peak observed at 1404.18 cm^{-1} is due to carboxylic acid's O-H bending, which was shifted to 1394.53 cm^{-1} in L-arginine-capped AgNPs. The C-O stretch peaks at 1128.36 cm^{-1} and 1178.51 cm^{-1} disappeared and were replaced by stretching of C-N at 1111 cm^{-1}, which means there is an interaction between L-arginine-coated AgNPs and is inconsistent with the previous study [39].

SEM Analysis

The shape of the nanoparticles generated through the biological method exhibited variation based on the reduction process. As illustrated in Fig. 3A,B, these nanoparticles were predominantly spherical, with aggregation occur-

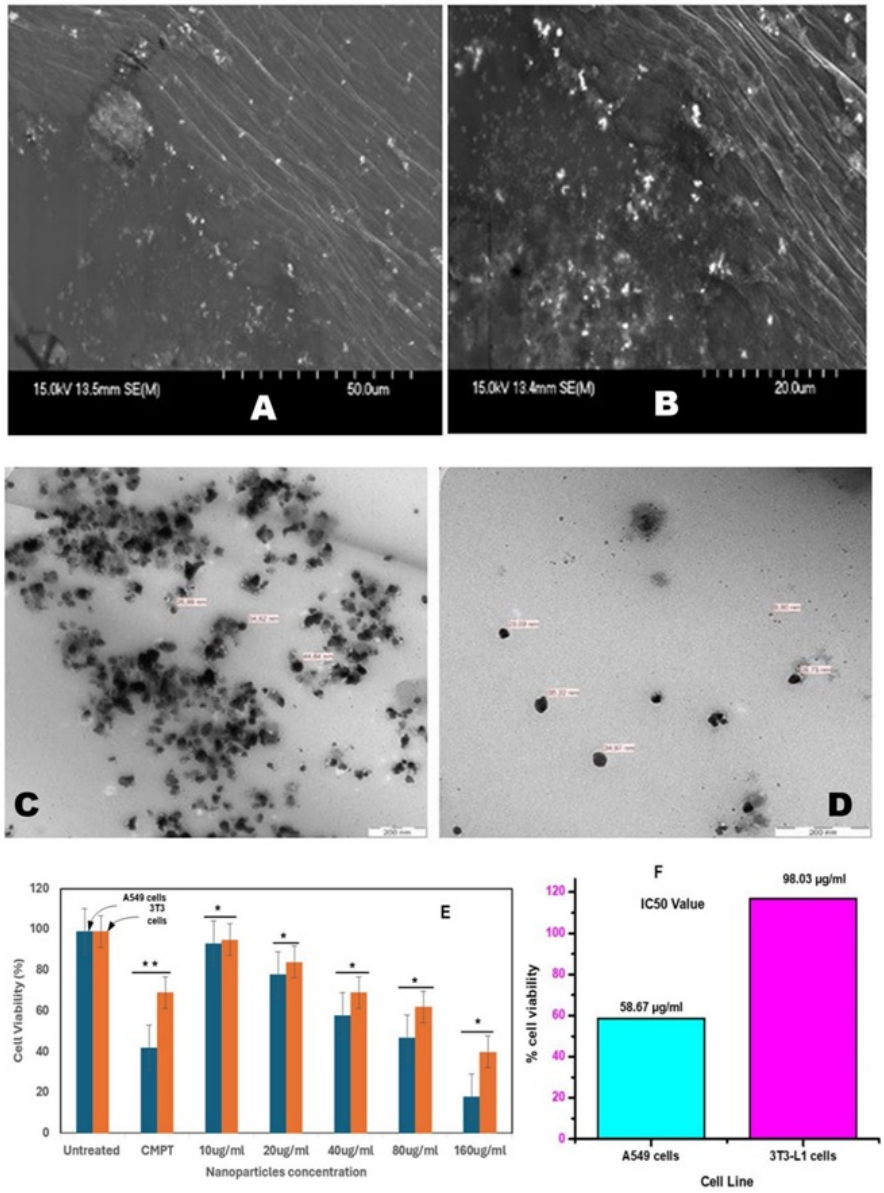

Fig. 3. Microscopic examination of nanoparticle. SEM images of L-AgNPs showing the surface topology of the nanoparticles (A,B) while (C,D) are TEM images of L-AgNPs at 200 nm scale, (E,F) are the Overlay of toxicity evaluation of L-AgNPs showing the cell viability upon using different concentrations shown in (A). $^{**}p < 0.01$ and $^{*}p < 0.05$ and half maximal inhibitory concentration (IC_{50}) value on A549 and 3T3-L1 cells treated with L-AgNPs shown in (F). SEM, Scanning Electron Microscopy; TEM, Transmission Electron Microscopy.

ring in multiple locations, and as individual particles in certain areas. The electrostatic interface between nanoparticle surface layers may have caused the nanoparticles to clump and stick together [40]. Nanoparticles also clump in suspension because of their large surface-area-to-volume ratio [41].

EDX Analysis

Elemental analysis of the L-AgNPs was accomplished by EDX, as illustrated in Fig. 4. The presence of silver in the compound was verified by EDX analysis. Two dominant signals were observed at approximately 3 keV in the EDX spectra, indicating the pure AgNPs [42]. The observable prominence of the silver peak is a consequence of the immersion of silver, which is prompted by the phenomenon of plasmon surface resonance [43]. According to Fig. 4, silver, oxygen, carbon, sodium, and gold weight percentages were 39.18, 19.37, 18.73, 12.37, and 10.35 per cent, respectively. The gold element was ascribed to the gold coating during SEM characterisation. Additional organic compounds like

Journal of
BIOLOGICAL REGULATORS
and Homeostatic Agents

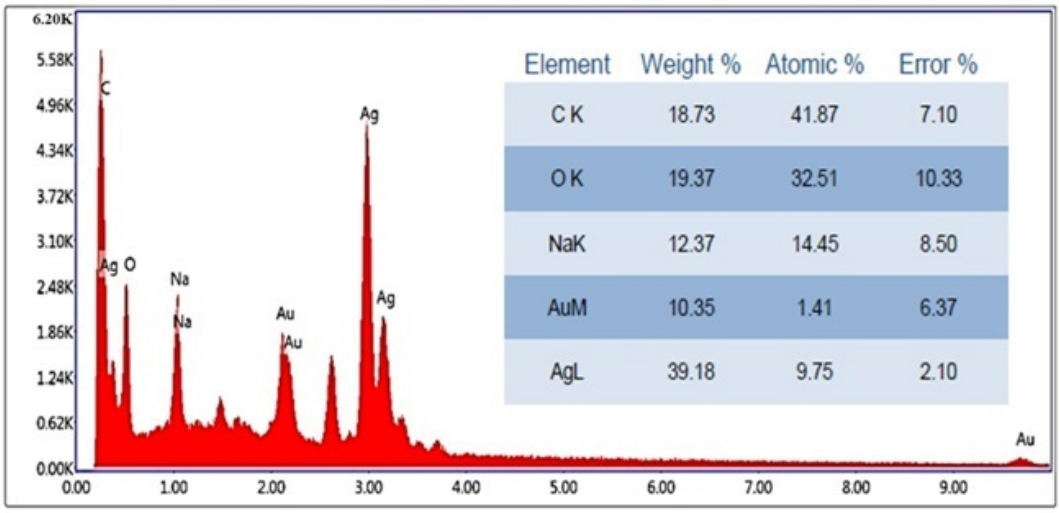

Fig. 4. EDX analysis of L-AgNPs showing the elemental nature of silver nanoparticles and also confirms the presence of silver. EDX, Energy-Dispersive X-ray Spectroscopy.

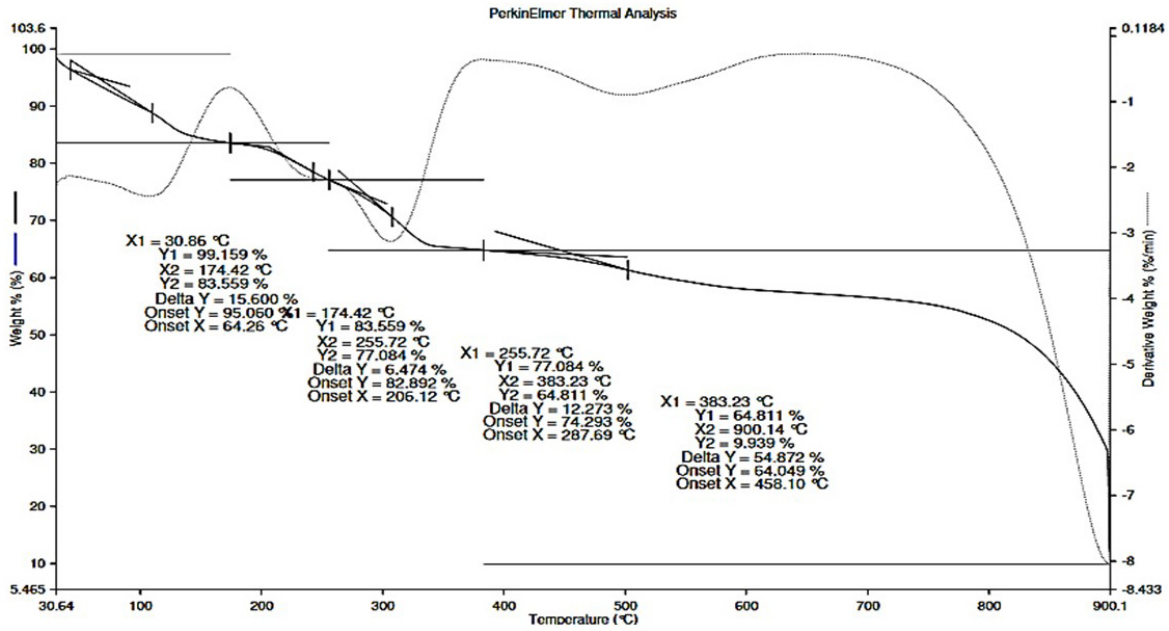

Fig. 5. Thermal Gravimetric Analysis (TGA) analysis of L-AgNPs at distinct temperatures.

O, C, and Na could either be attributed to the surface capping of silver nanoparticles or originated from the surrounding atmospheric environment.

TEM Analysis

The shape, distribution, and size of nanoparticles were measured using TEM. As depicted in Fig. 3C,D synthesized L-AgNPs exhibited predominantly spherical morphology, with a size distribution ranging from 8.8 nm to 44.6 nm with a mean diameter of 29.5 mm. Due to their diminutive size, the enormous surface-area-to-volume ratio exhibited by nanoparticles enables them to engage with biological molecules and elicit favorable outcomes effectively. Therefore, the physical characteristics of objects are of utmost importance in determining their functionalities within the biomedical domain, consistent with previous study [44].

TGA Analysis

TGA can be utilized to inspect alterations in the mass of nanoparticles at different temperatures [45] along with the amount of coatings on nanoparticles [46]. L-AgNPs were tested from 30.64 °C to 909.1 °C. The TGA curve demonstrated, at 30.86 °C, that the initial amount of sample was 99.15%, with a weight reduction of 15.6%; thus, the final sample amount was 83.55%. Water and organic solvent molecules escaping from the sample are thought to be

Table 1. Average inhibition zone of the Capped and Non-capped silver nanoparticles against various bacterial strains.

Pathogens	Inhibition zone											
	10 µg/µL		*p*	20 µg/µL		*p*	30 µg/µL		*p*	40 µg/µL		*p*	Control
	N	C		N	C		N	C		N	C		
Salmonella spp.	10.7 ± 0.9	11.3 ± 0.9	=0.013	12.7 ± 0.9	13.3 ± 0.9	=0.013	14.7 ± 0.9	15.3 ± 0.9	=0.013	16.0 ± 0.0	18.7 ± 0.9	=0.012	45.3 ± 0.9
P. aeruginosa	8.7 ± 0.9	10.0 ± 1.6	=0.017	11.3 ± 0.9	12.0 ± 1.6	=0.002	14.0 ± 1.6	14.0 ± 1.6	=0.292	16.0 ± 1.6	16.7 ± 0.9	0.028	28.7 ± 0.9
Bacillus cereus	8.7 ± 0.9	8.7 ± 0.9	>0.99	10.7 ± 0.9	10.0 ± 0.0	=0.010	12.7 ± 0.9	12.0 ± 0.0	=0.007	14.7 ± 0.9	14.0 ± 0.0	=0.101	31.3 ± 0.9
S. aureus	11.3 ± 0.9	10.0 ± 0.0	=0.003	13.3 ± 0.9	12.7 ± 0.9	=0.013	14.7 ± 0.9	14.7 ± 0.9	=0.292	16.7 ± 0.9	16.7 ± 0.9	=0.292	30.0 ± 0.0

C, L-arginine-capped AgNPs; N, Non-capped AgNPs. Experiment repeated as triplicate, mean ± Standard deviation (SD) was estimated and, $p < 0.05$ was considered statistically significant.

Table 2. Synergistic effects of capped silver nanoparticles and antibiotics.

Pathogens	Inhibition zone														
	Gentamicin (G)	G + L-AgNPs	*p*	Erythromycin (E)	E + L-AgNPs	*p*	Meropenem (M)	M + L-AgNPs	*p*	Cefotaxime (C)	C + L-AgNPs	*p*	Tetracycline (T)	T + L-AgNPs	*p*
S.aureus	23 ± 0.76	25 ± 0.85	=0.003	11 ± 0.62	14 ± 0.75	<0.0001	15 ± 0.60	16 ± 0.71	<0.0001	6 ± 0.9	12 ± 0.98	<0.0001	9 ± 1.2	13 ± 1.5	$p < 0.0001$
P. aeruginosa	24 ± 0.5	25 ± 0.62	=0.0002	NA	10 ± 0.7	NA	38 ± 0.82	39 ± 0.74	$p = 0.0004$	12 ± 0.87	14 ± 0.98	$p < 0.0001$	19 ± 0.5	19 ± 0.56	=0.50
B. cereus	19 ± 0.4	27 ± 0.9	=0.001	27 ± 1.2	28 ± 1.8	=0.0961	32 ± 0.32	34 ± 0.52	<0.0001	16 ± 0.65	20 ± 0.85	<0.0001	27 ± 0.9	31 ± 1.6	=0.0010
Salmonella spp.	25 ± 1.8	28 ± 1.8	=0.009	26 ± 0.4	28 ± 0.63	=0.059	34 ± 0.36	39 ± 0.42	<0.0001	33 ± 0.62	40 ± 0.82	=0.9439	34 ± 0.62	36 ± 0.84	<0.0001

NA, Not available. Experiment repeated as triplicate, mean ± SD was estimated and, $p < 0.05$ was considered statistically significant. G, Gentamicin; E, Erythromycin; M, Meropenem; C, Cefotaxime; T, Tetracycline.

Journal of
BIOLOGICAL REGULATORS
and Homeostatic Agents

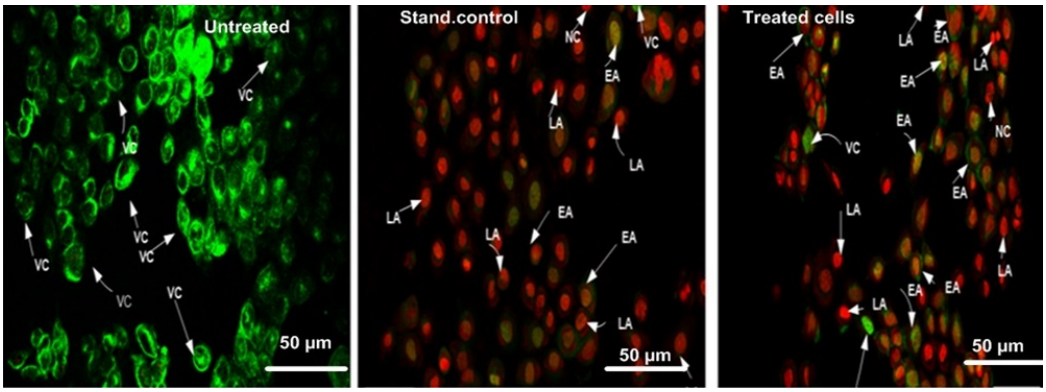

Fig. 6. Apoptosis induced by the L-AgNPs on A549 cells showing morphological change, cell shrinkage, and membrane blebbing in the cells. VC, Viable cells; NC, Necrotic cells; EA, Early apoptotic cells; LA, Late apoptotic cells.

liable for initial weight loss [47]. At 174.42 °C, the sample displayed was 83.55%, the weight loss was 6.47%, and the remaining sample was 77.08%. At 255.72 °C, the sample weight was displayed on the TGA curve, with a weight loss of 12.27%, leaving a 64.81% sample. At 383.23 °C, the TGA curve represented a sample quantity of 64.81%, and 54.87%; hence, the remaining sample weight was 9.93%. As per Fig. 5, starting from a temperature of 174.42 °C, it can be presumed that weight loss increases as heating temperature increases.

Antibacterial Activity of Capped and Non-Capped AgNPs

The antibacterial activity of both AgNPs and L-AgNPs was evaluated using the disc diffusion technique against clinically isolated *Bacillus cereus*, *Staphylococcus aureus* (ATCC 33682), *Salmonella typhi*, and *Pseudomonas aeruginosa* (ATCC 9022) at concentrations of 10–40 µg/µL. Both AgNPs and L-AgNPs exhibited a minimum zone of inhibition at 10 µg/µL and a maximum zone of inhibition at 40 µg/µL. At a concentration of 40 µg/µL, L-AgNPs demonstrated the highest inhibition zone against *Salmonella sp*., while AgNPs demonstrated the maximum inhibition zone against *Staphylococcus aureus*. At 10 µg/µL, L-AgNPs displayed the lowest inhibition zone against *Bacillus cereus*, and AgNPs displayed the lowest inhibition zone against *Bacillus cereus* and *Pseudomonas aeruginosa*. However the capped nanoparticles were not statistically significant as detailed in Table 1. Previous research has demonstrated that arginine-rich peptides possess potent antibacterial properties [48] due to the interaction of positively charged arginine peptides with negatively charged bacterial membranes [49]. Overall, both AgNPs and L-AgNPs showed an increase in antibacterial activity with increasing concentration. This finding is supported by research that confirmed that Ag^{+} is essential for bacterial death as it can instantly adsorb most biomolecules in bacteria [50].

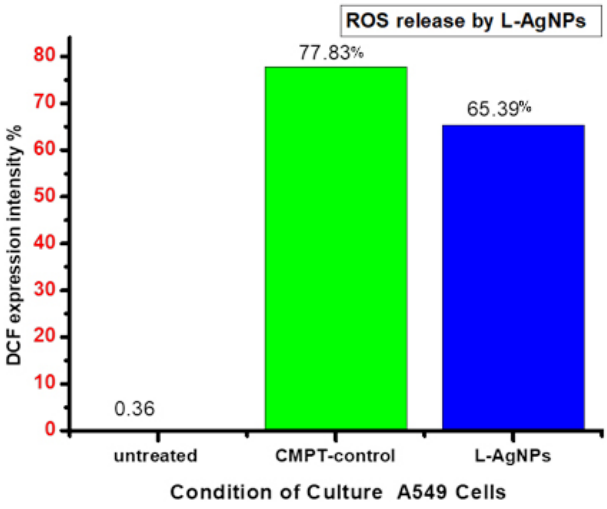

Fig. 7. Overlay of ROS release by the A549 cells treated with L-AgNPs showing the DCF expression at the M2 region. Camptothecin standard showed 77.83% and L-AgNPs 65.39% respectively. ROS, reactive oxygen species; DCF, dichlorodihydrofluorescein.

Combined Effects of L-AgNPs and Antibiotics

The synergistic effects of L-arginine-capped AgNPs with various antibiotics was assessed through disc diffusion method using 20 µg/mL of AgNPs against *Bacillus cereus*, *Staphylococcus aureus*, *Pseudomonas aeruginosa* and *Salmonella* spp. in 10 µg gentamicin, 10 µg meropenem, 5 µg cefotaxime, 30 µg tetracycline and 15 µg erythromycin were used as displayed in Table 2. The use of L-AgNPs in combination with antibiotics has demonstrated synergistic effects in the inhibition of *Bacillus cereus*, with mixtures of L-AgNPs and gentamicin displaying increased zones of inhibition with p value less than 0.001 compared to antibiotic action alone. Additionally, the combination of L-AgNPs and cefotaxime showed slight synergistic effects against *Salmonella* spp. (p = 0.9439). However, erythromycin had no antibacterial action against *P. aerug-*

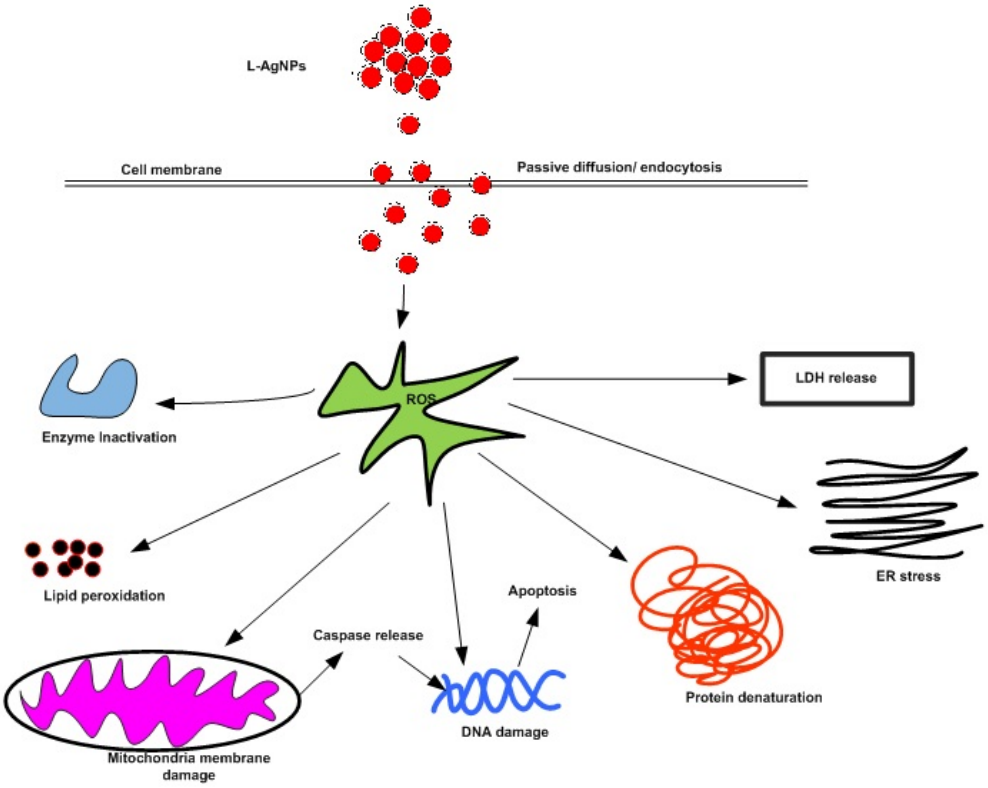

Fig. 8. Possible mechanism of L-AgNPs on cancer cells. (Created using Microsoft Visio 2007, Microsoft, Redmond, WA, USA). LDH, Lactate dehydrogenase.

inosa, but a substantial synergistic effect between erythromycin and L-AgNPs was observed, with an increased zone of inhibition compared to L-AgNPs alone as this bacteria is resistant to the antibiotics, however upon addition of L-arginine nanoparticles the zone of inhibition increased. One study has suggested that silver in dissolved ions attacks bacterial cells by permeating membrane surfaces or disrupting cell metabolism [51]. All combinations of L-AgNPs and antibiotics showed increased zones of inhibition, with cefotaxime ($p < 0.001$) demonstrating the most remarkable synergistic effect when combined with L-AgNPs, followed by gentamicin, erythromycin, and other antibiotics against specific bacteria.

Cytotoxic Analysis

Toxicity analysis was executed through MTT assay against A549 lung carcinoma cells. L-AgNPs were used as positive control at diverse concentrations (10, 20, 40, 80, and 160 µg/mL), along with camptothecin (10 µM/mL). These L-AgNPs exhibited good toxicity towards malignant cells with an IC_{50} of 58.67 µg/mL as shown in Fig. 3. Previous research has documented that, bacterial and fungal-generated AgNPs exhibit excellent anticancer properties against cancer cells of breast tissue [52]. Use of silver nanoparticles conjugated with peptides is a promising approach in nanomedicine, wherein these nanoparticles might serve as efficient carriers for delivering therapeutic drugs specifically to cancer cells. This targeted delivery system promises to minimize drug toxicity towards healthy cells [53]. Chitosan-conjugated silver nanoparticles induce toxicity towards cancer cells at minimal concentrations because of high ROS levels in HT29 cells [26].

In addition, L-AgNPs were contrasted with normal 3T3-L1 cell lines, with an IC_{50} of 98.03 µg/mL as indicated in Fig. 3E,F. A previous report showed that AgNPs produced from plants are highly toxic to malignant cells and relatively less toxic to healthy cells [53]. The enhanced toxicity of L-AgNPs towards cancer cells is due to the smaller shape and even distribution of the nanoparticles, and arginine enhances the penetration of cancer cells. Moreover, it was noticed that toxicity towards normal cells was minimal owing to the reduced expression of receptors in normal cells. Another study also demonstrated that biologically synthesized AgNPs are highly toxic to MCF7 and T47D cancer cells but exhibit reduced toxicity towards normal MCF-10A cells [54]. Therefore, our results are supported and in line with previous studies.

Evaluation of Apoptotic Activity

Death of A549 cancer cells was assessed utilizing acridine orange and ethidium bromide staining. Structural alterations were examined in cells treated with IC_{50} concentrations of L-AgNPs. Our findings suggest that cells exposed to L-AgNPs exhibited membrane blebbing,

Journal of
BIOLOGICAL REGULATORS
and Homeostatic Agents

chromatin condensation, and cell shrinkage as depicted in Fig. 6. The red-coloured cells confirmed apoptotic remanent, while orange-coloured cells showed necrosis in the treated cells when assessed against positive control. Previous research has demonstrated that AgNPs can cause apoptosis and that these particles are cytotoxic and highly specific to cancer cells [55]. The synthesis of AgNPs from *Nepeta deflersiana* plants triggered apoptosis in HeLa cells caused by necrosis and cell cycle blockage at the Sub G1 phase [56]. Reportedly, AgNPs stimulate the typical functioning of cell membranes by triggering the apoptotic genes within cells, ultimately resulting in cell death [53]. Therefore, our results are supported and in line with previous studies.

The lung cancer A549 cells were evaluated for ROS generation-induced oxidative stress C_{50} of L-AgNPs and contrasted against camptothecin (10 µm/mL) positive control. Findings confirm that L-AgNPs produced 65.39% dichlorodihydrofluorescein (DCF), while camptothecin showed 77.83% DCF intensity in the M2 region (Fig. 7). Therefore, L-AgNPs induced ROS and oxidative stress in lung cancer cells causing cell death. AgNPs induce apoptosis by producing ROS that exhibits antitumour, antiangiogenesis, and antiproliferative activities [57]. Furthermore, AgNPs induce the apoptotic gene signaling pathway, triggering cellular death [53].

The proposed process by which L-AgNPs inhibition induces cell death in cancer cells is illustrated in Fig. 8. ROS production causes mitochondrial membrane damage, which induces cellular toxicity [58]. A previous study also showed that AgNPs induce apoptosis through oxidative stress, causing mitochondrial membrane damage and enhanced ROS level, leading to DNA damage in human glioblastoma cells, whereas these were reported to have lower sensitivity to normal lung fibroblast cells [59]. Another study also showed that AgNPs disrupt DNA integrity in human colonic carcinoma cells [60]. AgNPs also upregulate the apoptotic gene *p53* which activates cytochrome C and releases caspase 9, which induces caspase 3 and apoptosis by changing cell morphology, chromatin condensation, and DNA damage [61]. Therefore, our study showed induce bacterial and malignant cell death due to oxidative stress induced by L-AgNPs, generating ROS that induce cellular damage via mitochondrial membrane damage and DNA fragmentation, which agrees with earlier research findings.

Conclusion

To conclude, *E. coli* proved effective in producing AgNPs. These AgNPs were then coated with L-arginine, and microscopic analysis confirmed their stability, spherical shape, and presence within the nano-size range. L-AgNPs exhibited notable antibacterial properties, as well as synergistic effects. When tested against A549 lung cancer cells, L-AgNPs demonstrated significant toxicity, while their impact on normal 3T3 cells was comparatively lower. Examination of cell apoptosis revealed characteristics such as shrinkage of cells, blebbing of membrane, and chromatin condensation. Furthermore, L-AgNPs generated substantial ROS release through oxidative stress, as evidenced by the heightened DCF intensity. As a result, these nanoparticles hold promise for potential use in anticancer therapy. However, it is crucial to conduct further investigations to assess their potential harm to healthy cells both *in vitro* and *in vivo*.

Availability of Data and Materials

All the data used to support the findings of this study are included within the article.

Author Contributions

KIMBN: investigation, data curation; writing original draft; SM, MSH and RM: data curation, editing; MD, SPS: methodology, data curation and proof editing; AMA, MNMI: resources, data curation; MTA: formal analysis and proof reading; SA, MAZ: investigation, methodology, data curation, editing and writing the initial manuscript; NHA, ERK and MSH: preparation of rough manuscript and final analysis of data. All authors made significant contributions to the idea or design of the study. All authors contributed to important editorial changes in the manuscript. All authors read and approved the final manuscript. All authors have participated sufficiently in the work and agreed to be accountable for all aspects of the work.

Ethics Approval and Consent to Participate

Not applicable.

Acknowledgment

Authors would like thank School of Chemical Sciences and School of Bioresource Technology Universiti Sains Malaysia for providing characterization facilities for this study.

Funding

This work was funded by Researchers Supporting Project number (RSP2024R26), King Saud University, Riyadh, Saudi Arabia. Princess Nourah bint Abdulrahman University Researchers Supporting Project number (PNURSP2024R62), Princess Nourah bint Abdulrahman University, Riyadh, Saudi Arabia. This work was also funded by Centre of Research and Innovation Universiti Kuala Lumpur Royal College of Medicine Perak, Malaysia (UniKL/CoRI/str21038).

Conflict of Interest

The authors declare no conflict of interest.

References

[1] Kesharwani P, Gorain B, Low SY, Tan SA, Ling ECS, Lim YK, *et al*. Nanotechnology based approaches for anti-diabetic drugs delivery. Diabetes Research and Clinical Practice. 2018; 136: 52–77.

[2] Prestinaci F, Pezzotti P, Pantosti A. Antimicrobial resistance: a global multifaceted phenomenon. Pathogens and Global Health. 2015; 109: 309–318.

[3] Beyth N, Houri-Haddad Y, Domb A, Khan W, Hazan R. Alternative antimicrobial approach: nano-antimicrobial materials. Evidence-based Complementary and Alternative Medicine: ECAM. 2015; 2015: 246012.

[4] Mba IE, Nweze EI. Nanoparticles as therapeutic options for treating multidrug-resistant bacteria: research progress, challenges, and prospects. World Journal of Microbiology & Biotechnology. 2021; 37: 108.

[5] Sánchez-López E, Gomes D, Esteruelas G, Bonilla L, Lopez-Machado AL, Galindo R, *et al*. Metal-Based Nanoparticles as Antimicrobial Agents: An Overview. Nanomaterials (Basel, Switzerland). 2020; 10: 292.

[6] White V PR. Respiratory disease. In Feather A, Randall D, Waterhouse M (eds.) Kumar and Clark's Clinical Medicine E-Book (pp. 927–999). Elsevier Health Sciences. 2020.

[7] Board PDQATE. Non-Small Cell Lung Cancer Treatment (PDQ®): Health Professional Version. PDQ Cancer Information Summaries. Bethesda (MD): National Cancer Institute (US). 2002.

[8] NSCLC Meta-Analyses Collaborative Group. Chemotherapy in addition to supportive care improves survival in advanced non-small-cell lung cancer: a systematic review and meta-analysis of individual patient data from 16 randomized controlled trials. Journal of Clinical Oncology: Official Journal of the American Society of Clinical Oncology. 2008; 26: 4617–4625.

[9] O'Rourke N, Roqué I Figuls M, FarréBernadó N, Macbeth F. Concurrent chemoradiotherapy in non-small cell lung cancer. The Cochrane Database of Systematic Reviews. 2010; CD002140.

[10] Rueth NM, Andrade RS. Is VATS lobectomy better: perioperatively, biologically and oncologically? The Annals of Thoracic Surgery. 2010; 89: S2107–S2111.

[11] Airley R. Cancer chemotherapy: basic science to the clinic. John Wiley & Sons. 2009.

[12] Păduraru DN, Ion D, Niculescu AG, Mușat F, Andronic O, Grumezescu AM, *et al*. Recent Developments in Metallic Nanomaterials for Cancer Therapy, Diagnosing and Imaging Applications. Pharmaceutics. 2022; 14: 435.

[13] Krishnan PD, Banas D, Durai RD, Kabanov D, Hosnedlova B, Kepinska M, *et al*. Silver Nanomaterials for Wound Dressing Applications. Pharmaceutics. 2020; 12: 821.

[14] Gomathi AC, Xavier Rajarathinam SR, Mohammed Sadiq A, Rajeshkumar S. Anticancer activity of silver nanoparticles synthesized using aqueous fruit shell extract of Tamarindus indica on MCF-7 human breast cancer cell line. Journal of Drug Delivery Science and Technology. 2020; 55: 101376.

[15] Lara HH, Ayala-Núñez NV, IxtepanTurrentLdC, Rodríguez Padilla C. Bactericidal effect of silver nanoparticles against multidrug-resistant bacteria. World Journal of Microbiology and Biotechnology. 2009; 26: 615–621.

[16] Talapko J, Matijević T, Juzbašić M, Antolović-Požgain A, Škrlec I. Antibacterial Activity of Silver and Its Application in Dentistry, Cardiology and Dermatology. Microorganisms. 2020; 8: 1400.

[17] Javed R, Zia M, Naz S, Aisida SO, Ain NU, Ao Q. Role of capping agents in the application of nanoparticles in biomedicine and environmental remediation: recent trends and future prospects. Journal of Nanobiotechnology. 2020; 18: 172.

[18] Ajitha B, Kumar Reddy YA, Reddy PS, Jeon H-J, Ahn CW. Role of capping agents in controlling silver nanoparticles size, antibacterial activity and potential application as optical hydrogen peroxide sensor. RSC Advances. 2016; 6: 36171–36179.

[19] Sidhu AK, Verma N, Kaushal P. Role of Biogenic Capping Agents in the Synthesis of Metallic Nanoparticles and Evaluation of Their Therapeutic Potential. Frontiers in Nanotechnology. 2022; 3.

[20] Gautam YK, Sharma K, Tyagi S, Kumar A, Singh BP. Applications of green nanomaterials in coatings. Green Nanomaterials for Industrial Applications: Elsevier. 2022; 107–152.

[21] Zhang XF, Liu ZG, Shen W, Gurunathan S. Silver Nanoparticles: Synthesis, Characterization, Properties, Applications, and Therapeutic Approaches. International Journal of Molecular Sciences. 2016; 17: 1534.

[22] Ali I, Qiang TY, Ilahi N, Adnan M, Sajjad W. Green synthesis of silver nanoparticles by using bacterial extract and its antimicrobial activity against pathogens. International Journal of Biosciences (IJB). 2018; 13: 113–127.

[23] Rai MK, Deshmukh SD, Ingle AP, Gade AK. Silver nanoparticles: the powerful nanoweapon against multidrug-resistant bacteria. Journal of Applied Microbiology. 2012; 112: 841–852.

[24] Gurunathan S, Han JW, Dayem AA, Eppakayala V, Park JH, Cho SG, *et al*. Green synthesis of anisotropic silver nanoparticles and its potential cytotoxicity in human breast cancer cells (MCF-7). Journal of Industrial and Engineering Chemistry. 2013; 19: 1600–1605.

[25] Gurunathan S, Han JW, Eppakayala V, Jeyaraj M, Kim JH. Cytotoxicity of biologically synthesized silver nanoparticles in MDA-MB-231 human breast cancer cells. BioMed Research International. 2013; 2013: 535796.

[26] Nosrati H, Abbasi R, Charmi J, Rakhshbahar A, Aliakbarzadeh F, Danafar H, *et al*. Folic acid conjugated bovine serum albumin: An efficient smart and tumor targeted biomacromolecule for inhibition folate receptor positive cancer cells. International Journal of Biological Macromolecules. 2018; 117: 1125–1132.

[27] Mohanta YK, Behera SK. Biosynthesis, characterization and antimicrobial activity of silver nanoparticles by Streptomyces sp. SS2. Bioprocess and Biosystems Engineering. 2014; 37: 2263–2269.

[28] Clausen PA, Kofoed-Sørensen V, Nørgaard AW, Sahlgren NM, Jensen KA. Thermogravimetry and Mass Spectrometry of Extractable Organics from Manufactured Nanomaterials for Identification of Potential Coating Components. Materials (Basel, Switzerland). 2019; 12: 3657.

[29] Majeed S, Danish M, Binti Zahrudin AH, Dash GK. Biosynthesis and characterization of silver nanoparticles from fungal species and its antibacterial and anticancer effect. Karbala International Journal of Modern Science. 2018; 4: 86–92.

[30] Mourdikoudis S, Pallares RM, Thanh NTK. Characterization techniques for nanoparticles: comparison and complementarity upon studying nanoparticle properties. Nanoscale. 2018; 10: 12871–12934.

[31] Majeed S, Danish M, Zakariya NA, Hashim R, Ansari MT, Sisinthy SP. Tailored silver nanoparticles capped with gallic acid and its potential toxicity via ROS mediated pathway against osteosarcoma cells. Materials Today Communications. 2022; 32: 103844.

[32] Rashid S, Azeem M, Khan SA, Shah MM, Ahmad R. Characterization and synergistic antibacterial potential of green synthesized silver nanoparticles using aqueous root extracts of im-

Journal of
BIOLOGICAL REGULATORS
and Homeostatic Agents

portant medicinal plants of Pakistan. Colloids and Surfaces. B, Biointerfaces. 2019; 179: 317–325.

[33] Alley MC, Scudiero DA, Monks A, Czerwinski M, Shoemaker R, Boyd MR. Validation of an automated microculture tetrazolium assay (MTA) to assess growth and drug sensitivity of human tumor cell lines. Proceedings of the American Association for Cancer Research. 1986; 27: 389.

[34] Gorman A, McCarthy J, Finucane D, Reville W. Morphological assessment of apoptosis. In TG Cotter, SJ Martin (eds.) Techniques in Apoptosis: A User's Guide. Portland Press: London. 1996.

[35] Chang HY, Huang HC, Huang TC, Yang PC, Wang YC, Juan HF. Flow Cytometric Detection of Reactive Oxygen Species. BIO-PROTOCOL. 2013; 3.

[36] Podila R, Chen R, Ke PC, Brown JM, Rao AM. Effects of surface functional groups on the formation of nanoparticle-protein corona. Applied Physics Letters. 2012; 101: 263701.

[37] Ravichandran S, Paluri V, Kumar G, Loganathan K, Kokati Venkata BR. A novel approach for the biosynthesis of silver oxide nanoparticles using aqueous leaf extract of*Callistemonlanceolatus*(Myrtaceae) and their therapeutic potential. Journal of Experimental Nanoscience. 2015; 11: 445–458.

[38] Wu F, Liu D, Wang T, Li W, Zhou X. Different surface properties of l-arginine functionalized silver nanoparticles and their influence on the conductive and adhesive properties of nanosilver films. Journal of Materials Science: Materials in Electronics. 2015; 26: 6781–6786.

[39] Yusefi M, Shameli K, Ali RR, Pang SW, Teow SY. Evaluating Anticancer Activity of Plant-Mediated Synthesized Iron Oxide Nanoparticles Using Punica Granatum Fruit Peel Extract. Journal of Molecular Structure. 2020; 1204: 127539.

[40] Bae E, Lee BC, Kim Y, Choi K, Yi J. Effect of agglomeration of silver nanoparticle on nanotoxicity depression. Korean Journal of Chemical Engineering. 2012; 30: 364–368.

[41] Mondal AH, Yadav D, Mitra S, Mukhopadhyay K. Biosynthesis of Silver Nanoparticles Using Culture Supernatant of *Shewanella* sp. ARY1 and Their Antibacterial Activity. International Journal of Nanomedicine. 2020; 15: 8295–8310.

[42] Majeed S, Danish M, Zakariya NA, Hashim R, Ansari MT, Alkahtani S, *et al*. In Vitro Evaluation of Antibacterial, Antioxidant, and Antidiabetic Activities and Glucose Uptake through 2-NBDG by Hep-2 Liver Cancer Cells Treated with Green Synthesized Silver Nanoparticles. Oxidative Medicine and Cellular Longevity. 2022; 2022: 1646687.

[43] Zakariya NA, Majeed S, Jusof WHW. Investigation of antioxidant and antibacterial activity of iron oxide nanoparticles (IONPS) synthesized from the aqueous extract of Penicillium spp. Sensors International. 2022; 3: 100164.

[44] Majeed S, Bakhtiar NFB, Danish M, Mohamad Ibrahim MN, Hashim R. Green approach for the biosynthesis of silver nanoparticles and its antibacterial and antitumor effect against osteoblast MG-63 and breast MCF-7 cancer cell lines. Sustainable Chemistry and Pharmacy. 2019; 12: 100138.

[45] Dongargaonkar AA, Clogston JD. Quantitation of Surface Coating on Nanoparticles Using Thermogravimetric Analysis. Methods in Molecular Biology (Clifton, N.J.). 2018; 1682: 57–63.

[46] Tamaekong N, Liewhiran C, Phanichphant S. Synthesis of Thermally Spherical CuO Nanoparticles. Journal of Nanomaterials. 2014; 2014: 1–5.

[47] Cutrona KJ, Kaufman BA, Figueroa DM, Elmore DE. Role of arginine and lysine in the antimicrobial mechanism of histone-derived antimicrobial peptides. FEBS Letters. 2015; 589: 3915–3920.

[48] Yang CH, Chen YC, Peng SY, Tsai APY, Lee TJF, Yen JH, *et al*. An engineered arginine-rich α-helical antimicrobial peptide exhibits broad-spectrum bactericidal activity against pathogenic bacteria and reduces bacterial infections in mice. Scientific Reports. 2018; 8: 14602.

[49] Xu Z, Zhang C, Wang X, Liu D. Release Strategies of Silver Ions from Materials for Bacterial Killing. ACS Applied Bio Materials. 2021; 4: 3985–3999.

[50] Morones-Ramirez JR, Winkler JA, Spina CS, Collins JJ. Silver enhances antibiotic activity against gram-negative bacteria. Science Translational Medicine. 2013; 5: 190ra81.

[51] Prasannaraj G, Venkatachalam P. Green engineering of biomolecule-coated metallic silver nanoparticles and their potential cytotoxic activity against cancer cell lines. Advances in Natural Sciences: Nanoscience and Nanotechnology. 2017; 8: 025001.

[52] Benyettou F, Rezgui R, Ravaux F, Jaber T, Blumer K, Jouiad M, *et al*. Synthesis of silver nanoparticles for the dual delivery of doxorubicin and alendronate to cancer cells. Journal of Materials Chemistry. B. 2015; 3: 7237–7245.

[53] Sanpui P, Chattopadhyay A, Ghosh SS. Induction of apoptosis in cancer cells at low silver nanoparticle concentrations using chitosan nanocarrier. ACS Applied Materials & Interfaces. 2011; 3: 218–228.

[54] Ortega FG, Fernández-Baldo MA, Fernández JG, Serrano MJ, Sanz MI, Diaz-Mochón JJ, *et al*. Study of antitumor activity in breast cell lines using silver nanoparticles produced by yeast. International Journal of Nanomedicine. 2015; 10: 2021–2031.

[55] Gopinath P, Gogoi SK, Chattopadhyay A, Ghosh SS. Implications of silver nanoparticle induced cell apoptosis for in vitro gene therapy. Nanotechnology. 2008; 19: 075104.

[56] Al-Sheddi ES, Farshori NN, Al-Oqail MM, Al-Massarani SM, Saquib Q, Wahab R, *et al*. Anticancer Potential of Green Synthesized Silver Nanoparticles Using Extract of *Nepeta deflersiana* against Human Cervical Cancer Cells (HeLA). Bioinorganic Chemistry and Applications. 2018; 2018: 9390784.

[57] Gurunathan S, Lee KJ, Kalishwaralal K, Sheikpranbabu S, Vaidyanathan R, Eom SH. Antiangiogenic properties of silver nanoparticles. Biomaterials. 2009; 30: 6341–6350.

[58] Dwivedi S, Siddiqui MA, Farshori NN, Ahamed M, Musarrat J, Al-Khedhairy AA. Synthesis, characterization and toxicological evaluation of iron oxide nanoparticles in human lung alveolar epithelial cells. Colloids and Surfaces. B, Biointerfaces. 2014; 122: 209–215.

[59] AshaRani PV, Low Kah Mun G, Hande MP, Valiyaveettil S. Cytotoxicity and genotoxicity of silver nanoparticles in human cells. ACS Nano. 2009; 3: 279–290.

[60] Dehghanizade S, Arasteh J, Mirzaie A. Green synthesis of silver nanoparticles using Anthemis atropatana extract: characterization and in vitro biological activities. Artificial Cells, Nanomedicine, and Biotechnology. 2018; 46: 160–168.

[61] Cai J, Yang J, Jones DP. Mitochondrial control of apoptosis: the role of cytochrome c. Biochimica et Biophysica Acta. 1998; 1366: 139–149.